Medical Hypotheses 122 (2019) 73–81

Contents lists available at ScienceDirect

Medical Hypotheses

journal homepage: www.elsevier.com/locate/mehy

Spatial gradient of *bicoid* is well explained by Birnbaum-Saunders distribution

Hossein Hassani*, Mahdi Kalantari, Zara Ghodsi

Department of Statistics, Payame Noor University, 19395–4697 Tehran, Iran

ARTICLE INFO

Keywords:
bicoid gene
Birnbaum-Saunders distribution
Drosophila melanogaster
Model
Segmentation gene

ABSTRACT

bicoid is a maternally transcribed gene which plays a pivotal role during the early developmental stage of *Drosophila melanogaster* by acting as an essential input to the segmentation network. Therefore, fundamental insights into gene cross-regulations of segmentation network expect to be unveiled by presenting an accurate mathematical model for *bicoid* gene expression profile. In this paper, an extended version of Birnbaum-Saunders with four parameters is introduced and evaluated to describe the spatial gradient of this gene. Theoretical aspects of four-parameter Birnbaum-Saunders and the estimated parameters are presented and thoroughly assessed for different embryos. The reliability and validity of the results are evaluated via both simulation studies and real data sets and thereby adding more confidence and value to the findings of this research.

1. Introduction

Birnbaum-Saunders (BS) distribution is an important fatigue-life model with non-negative support proposed by Birnbaum and Saunders [1]. Although BS distribution which is also known as fatigue life distribution was initially proposed for material fatigue and reliability analyses, the notable and attractive statistical and probabilistic properties of this model soon made BS as an excellent candidate and powerful technique in various fields of study such as earth, environmental and medical sciences; see for example [2–6].

In this paper, we provide a more in-depth understanding of BS distribution by introducing an extended version of this distribution with four parameters. Our interest in this topic is motivated by recent findings in [7] where authors proposed the BS distribution to describe the expression profile of *bicoid* gene. In that study, *bicoid* gene expression was described as a significantly stochastic and high volatile profile with a heavy tail. Following a thorough evaluation of fifty-four commonly used distributions, Hassani et al. concluded that BS distribution with three parameters fits the *bicoid* profile more accurately than the other distributions.

The protein encoded by *bicoid* gene is a homeodomain transcriptional factor whose concentration gradient plays a crucial role in forming the segmented pattern of *Drosophila melanogaster*. *bicoid* gradient controls the expression of all the other Hox genes by turning on the gap genes at different thresholds [8]. Gap genes, in turn, activate Hox genes in the same sequence as their 3′-to-5′ order [8,9].

Besides the fact that studies on certain characteristics of transcriptional factors initially started with studying *Drosophila melanogaster*, the main reason behind focusing on this model organism in genetic studies is an evolutionary principle stating that due to the common ancestry fact, all organisms have some degree of relatedness and genetic similarity. For example, several basic biological, physiological, and neurological characteristics are conserved between mammals and *Drosophila melanogaster*, and approximately 75% of human disease-causing genes are believed to have a functional homolog in this fly [10]. As can be seen in Fig. 1, in both cases of humans and flies, Hox genes impose “tagmosis”-regional identities (thoracic vs. lumbar in humans or thoracic vs. abdominal in flies) [8,11,12].

To introduce the extended version of BS model, extensive simulation studies have been carried out. Analysing the real data set have also been performed on all the cleavage cycles in which *bicoid* gene is expressed in the embryo.

Having performed the analysis on both simulated and real data sets, it was found that the four-parameter BS distribution (FBS) introduced in this study incorporates parameters and serves as a competitor to the commonly-used three-parameter counterpart [13].

The remainder of this paper is organized as follows. Section 2 provides a theoretical framework for BS distribution which is followed by Maximum Likelihood (ML) estimation of parameters and simulation study procedure. Section 3 describes the data set and evaluates the FBS on the real data. The paper concludes with a concise summary in Section 4.

* Corresponding author at: Research Institute of Energy Management and Planning (RIEMP), University of Tehran, Tehran 1417466191, Iran.

https://doi.org/10.1016/j.mehy.2018.10.023
Received 14 July 2018; Accepted 21 October 2018
0306-9877/

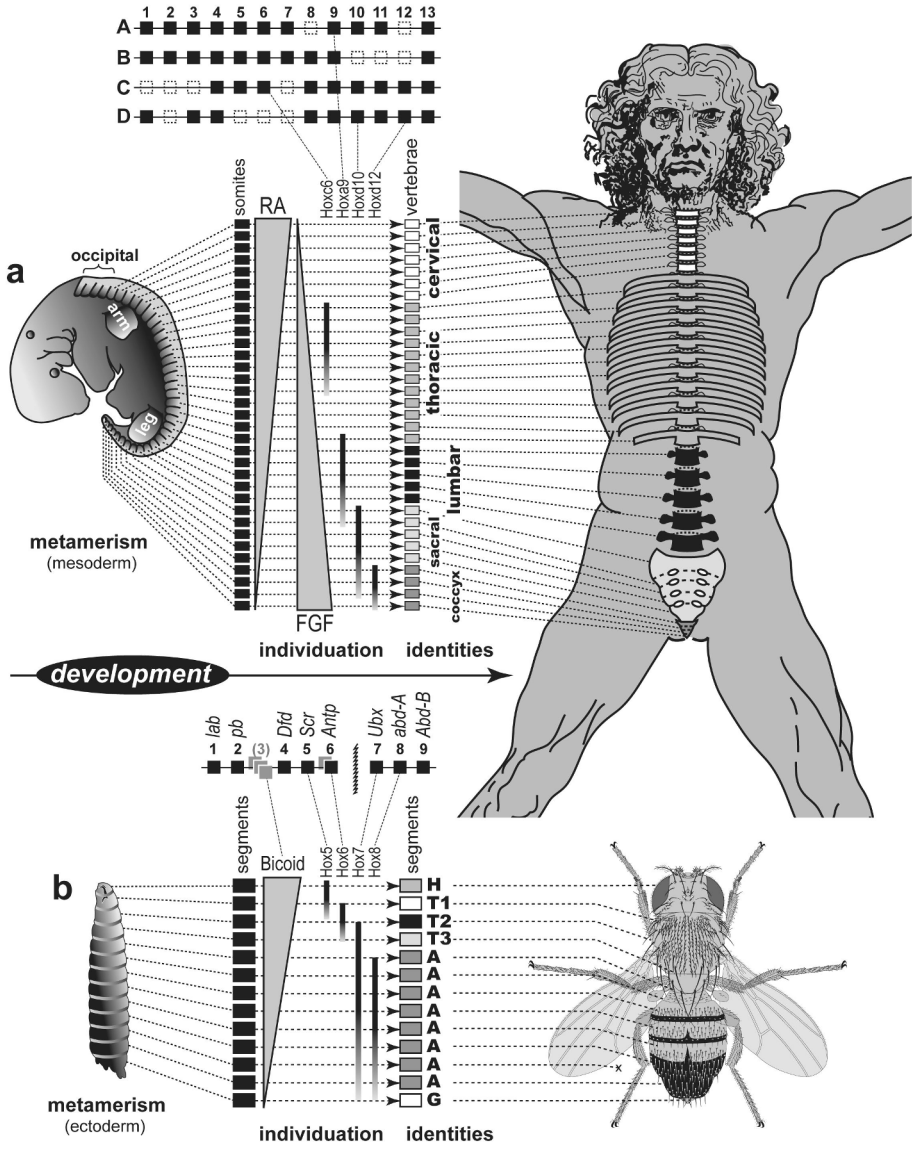

Fig. 1. Colinearity of Hox gene expression along the Anterior-posterior (A-P) axis in (a) humans and (b) flies. Figure adopted from [8].

2. Theoretical framework

In this section; first, the underlying theory of BS distribution is reviewed and then we propose the log-likelihood equations to obtain ML estimates of distribution parameters. We believe that knowing the parameters of this distribution such as the shape, scale and location parameter, would help to interpret and explore *bicoid* functioning as an initiator of segmentation network.

In order to evaluate the performance of FBS distribution in fitting to real *bicoid* expression profiles, we perform a simulation study by simulating the exponential curve drawn from the Synthesis Diffusion Degradation (SDD) model which is a common model for analysing the *bicoid* profile [14–17].

2.1. Birnbaum-Saunders distribution

The classical BS distribution originally proposed in [1] contains two parameters; shape (α) and scale (β). Particularly, the random variable $T$is said to follow the two-parameter BS distribution, denoted by $T \sim BS(\alpha, \beta)$, if its cumulative distribution function (cdf) is given by

$$F_T(t|\alpha, \beta) = \Phi\left(\frac{1}{\alpha}\left(\sqrt{\frac{t}{\beta}} - \sqrt{\frac{\beta}{t}}\right)\right), \quad t > 0, \quad \alpha, \beta > 0, \tag{1}$$

where $\Phi(\cdot)$is the cdf of standard normal distribution. This model has an interesting relationship with the standard normal distribution. If $T \sim BS(\alpha, \beta)$, then

$$Z = \frac{1}{\alpha}\left(\sqrt{\frac{T}{\beta}} - \sqrt{\frac{\beta}{T}}\right) \sim N(0, 1). \tag{2}$$

More detailed information on two-parameter BS distribution can be found in [18].

There is another type of BS distribution which includes three parameters [13]. The random variable Twhich follows the three-parameter BS distribution is denoted by $T \sim BS(\alpha, \mu, \beta)$and its cdf has the following form

$$F_T(t|\alpha, \mu, \beta) = \Phi\left(\frac{1}{\alpha}\left(\sqrt{\frac{t-\mu}{\beta}} - \sqrt{\frac{\beta}{t-\mu}}\right)\right), \quad t > \mu, \quad \alpha, \beta > 0, \quad \mu \in \mathbb{R}, \tag{3}$$

where the parameter μ represents the location of distribution. It is noteworthy that if $T \sim BS(\alpha, \mu, \beta)$, then

$$Z = \frac{1}{\alpha}\left(\sqrt{\frac{T-\mu}{\beta}} - \sqrt{\frac{\beta}{T-\mu}}\right) \sim N(0,1). \tag{4}$$

The BS distribution has been extended in [13] based on the Johnson System. The random variable T is said to follow the FBS distribution, denoted by $T \sim FBS(\delta, \lambda, \xi, \gamma)$, if its cdf is given by

$$F_T(t|\delta,\lambda,\xi,\gamma) = \Phi\left(\gamma + \delta\left(\sqrt{\frac{t-\xi}{\lambda}} - \sqrt{\frac{\lambda}{t-\xi}}\right)\right), \quad t > \xi, \quad \delta,\lambda > 0, \quad \xi,\gamma \in \mathbb{R}. \tag{5}$$

The parameters δ, λ, ξ and γ are the shape, scale, location and non centrality parameters, respectively. Similarly, if $T \sim FBS(\delta, \lambda, \xi, \gamma)$, then

$$Z = \gamma + \delta\left(\sqrt{\frac{T-\xi}{\lambda}} - \sqrt{\frac{\lambda}{T-\xi}}\right) \sim N(0,1). \tag{6}$$

It is evident that if $\gamma = \xi = 0$, then $T \sim BS(\alpha = 1/\delta, \beta = \lambda)$, and if $\gamma = 0$, $\xi = \mu$, then $T \sim BS(\alpha = 1/\delta, \mu = \xi, \beta = \lambda)$. Therefore, the FBS distribution contains all the versions as particular cases. As discussed in [13], the extra parameters make the classical BS distribution more flexible, thus widening the shape, form, characteristics and properties of the BS model.

2.2. Parameters estimation

Let $T_1, T_2, ..., T_n$ be a random sample of size n from the FBS distribution. The log-likelihood function for $\theta = (\delta, \lambda, \xi, \gamma)^T$ is given by

$$\begin{aligned} l(\theta) = {} & nc + n\log(\delta) - \frac{n}{2}\log(\lambda) - \frac{n}{2}\gamma^2 + n\delta^2 - \frac{\delta^2}{2}\left(\frac{g(\xi,1)}{\lambda} + \lambda g(\xi,-1)\right) \\ & - \delta\gamma\left(\frac{g\left(\xi,\frac{1}{2}\right)}{\sqrt{\lambda}} - \sqrt{\lambda}g\left(\xi,\frac{-1}{2}\right)\right) - \frac{3}{2}\sum_{i=1}^{n}\log(t_i-\xi) \\ & + \sum_{i=1}^{n}\log(t_i-\xi+\lambda), \end{aligned} \tag{7}$$

where $t_1, t_2, ..., t_n$ is observed sample, $c = \frac{-1}{2}\log(2\pi) - \log(2)$ is a constant that does not depend on θ, and the function g is defined as

$$g(\xi, p) = \sum_{i=1}^{n}(t_i - \xi)^p. \tag{8}$$

It is evident that $g(\xi, 0) = n$ and $\frac{\partial g(\xi,p)}{\partial \xi} = -pg(\xi, p-1)$ by (8). Now, by getting the partial derivatives of $l(\theta)$, the log-likelihood equations can be obtained as follows:

$$\begin{aligned} & \frac{n}{\delta} + 2n\delta - \delta\left(\frac{g(\xi,1)}{\lambda} + \lambda g(\xi,-1)\right) - \gamma\left(\frac{g\left(\xi,\frac{1}{2}\right)}{\sqrt{\lambda}} - \sqrt{\lambda}g\left(\xi,\frac{-1}{2}\right)\right) = 0 \\ & \frac{-n}{2\lambda} + \frac{\delta^2}{2}\left(\frac{g(\xi,1)}{\lambda^2} - g(\xi,-1)\right) + \frac{\delta\gamma}{2\sqrt{\lambda}}\left(\frac{g\left(\xi,\frac{1}{2}\right)}{\lambda} + g\left(\xi,\frac{-1}{2}\right)\right) \\ & \qquad + \sum_{i=1}^{n}(t_i-\xi+\lambda)^{-1} = 0 \\ & \frac{n\delta^2}{2\lambda} - \frac{\lambda\delta^2}{2}g(\xi,-2) + \frac{\delta\gamma}{2\sqrt{\lambda}}g\left(\xi,\frac{-1}{2}\right) + \frac{\delta\gamma\sqrt{\lambda}}{2}g\left(\xi,\frac{-3}{2}\right) + \frac{3}{2}g(\xi,-1) \\ & \qquad - \sum_{i=1}^{n}(t_i-\xi+\lambda)^{-1} = 0 \\ & -n\gamma - \delta\left(\frac{g\left(\xi,\frac{1}{2}\right)}{\sqrt{\lambda}} - \sqrt{\lambda}g\left(\xi,\frac{-1}{2}\right)\right) = 0 \end{aligned} \tag{9}$$

These log-likelihood equations have no explicit solutions and therefore they should be solved by using numerical algorithms to get ML estimates.

Let us now use a series of simulated data to evaluate the performance of FBS distribution to describe the data. First, an exponential curve was drawn from the SDD model and then to obtain a noisy series, normally distributed random noise with zero mean and different amplitudes variance were added to various parts of the series. In total 100 observations were generated and the simulation was repeated 1000 times.

Here, the most widely accepted goodness of fit tests are adopted including Kolmogorov–Smirnov (KS) and Anderson–Darling (AD) tests. After each step of simulation, the p-values of these tests are considered as the criterion for decision making. Fig. 2(a) depicts the box plots for the value of test statistic for KS and AD tests. As can be seen in this

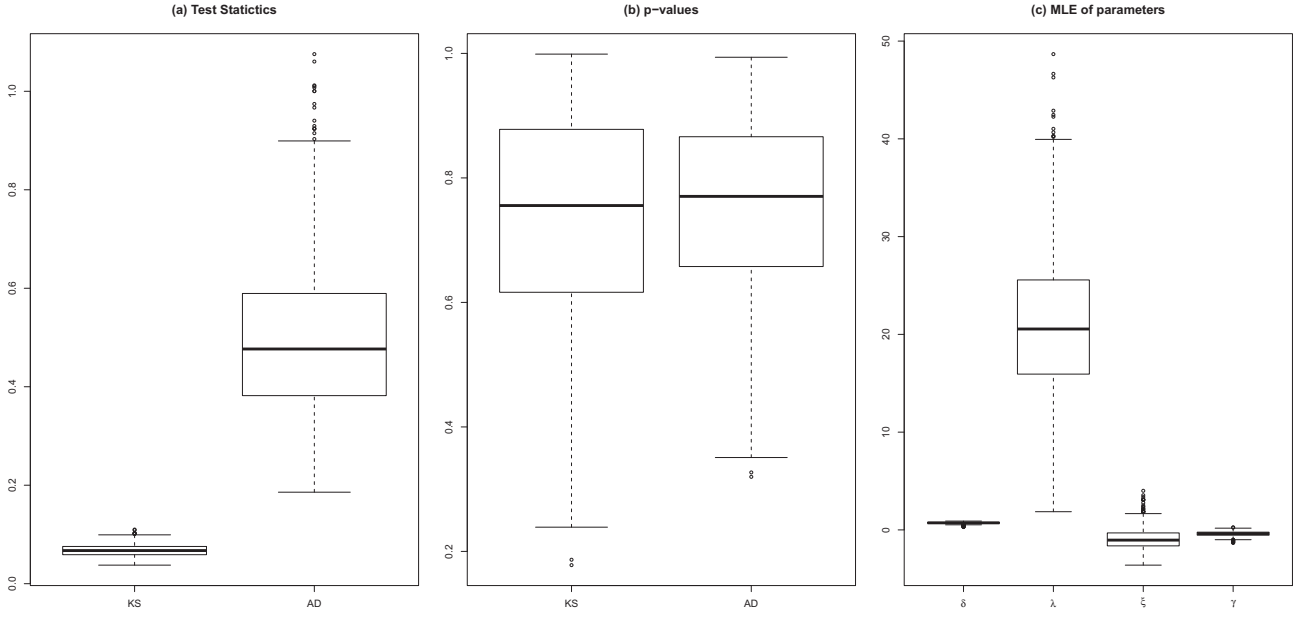

Fig. 2. The box plot of test statistics, p-values and MLE of parameters.

Table 1
Standard error of parameters in simulation study.

Parameter	δ	λ	ξ	γ
Standard error	0.083	7.457	1.075	0.239

figure, variation in the AD test statistic is greater than KS test statistic. Fig. 2(b) shows the box plots of p-value for KS and AD tests. The minimum of p-values is 0.178 and 0.32 in KS and AD tests, respectively. Therefore, it can be concluded that the FBS distribution fits to all simulated data. In Fig. 2(c), the box plot of ML estimated parameters is shown. Note that how the variation in scale parameter (λ) is much more than other parameters. In addition, the standard errors of ML parameter estimation reported in Table 1 indicate that the shape parameter (δ) has the lowest standard error and the standard error of location parameter (ξ) is greater than non centrality parameter (γ).

2.3. Hazard rate and TTT plot

The hazard rate is a fundamental concept in reliability theory and survival analysis. It is also known as failure rate, chance function or risk rate. Hazard rate is important factor in the insurance, finance, commerce and regulatory industries and fundamental to the design of safe systems in a wide variety of applications.

It is well known that the behavior of a statistical distribution can be characterized by hazard rate. If a distribution is absolutely continuous, the hazard rate uniquely determines it [19]. The hazard rate may be increasing, constant (exponential distribution), decreasing, ∪-shaped or bathtub, ∩-shaped or inverse bathtub, and upside-down bathtub [18].

In general, the hazard rate of random variable T is defined by

$$h_T(t) = \frac{f_T(t)}{1 - F_T(t)}, \tag{10}$$

where $f_T(\cdot)$ is the probability distribution function (pdf) of T and $F_T(\cdot)$ its cdf. The hazard rate of FBS distribution has been studied in [13]. If $T \sim FBS(\delta, \lambda, \xi, \gamma)$, then the hazard rate of T is given by

$$h_T(t) = \frac{\phi(a_t)}{\Phi(-a_t)} A_t, \quad t > \xi, \quad \delta, \lambda > 0, \quad \xi, \gamma \in \mathbb{R}, \tag{11}$$

where $\phi(\cdot)$ and $\Phi(\cdot)$ are pdf and cdf of standard normal distribution, respectively; and

$$a_t = \gamma + \delta\left(\sqrt{\frac{t-\xi}{\lambda}} - \sqrt{\frac{\lambda}{t-\xi}}\right) \tag{12}$$

$$A_t = \frac{da_t}{dt} = \frac{\delta(t-\xi)^{-\frac{3}{2}}(t-\xi+\lambda)}{2\sqrt{\lambda}} \tag{13}$$

The hazard rate of FBS distribution has a variety of shapes depending on the values of FBS parameters. For instance, in the case of $\gamma = 0$ which is the three parameters BS distribution, the hazard rate has inverse bathtub shape [13].

The Total Time on Test (TTT) function is a useful tool to characterize the shape of the hazard rate [19]. This function and its scaled version are defined as follows

$$H_T^{-1}(u) = \int_0^{F_T^{-1}(u)} (1 - F_T(y))dy, \tag{14}$$

$$W_T(u) = \frac{H_T^{-1}(u)}{H_T^{-1}(1)}, \quad 0 < u < 1. \tag{15}$$

The scaled TTT function can be approximated by empirical version of it which is defined as

$$W_n\left(\frac{k}{n}\right) = \frac{\sum_{i=1}^{k} T_{(i)} + (n-k)T_{(k)}}{\sum_{i=1}^{n} T_{(i)}}, \quad k = 0, \ldots, n, \tag{16}$$

where $T_{(i)}$ is ith order statistic. Plotting the consecutive points $(k/n, W_n(k/n))$ gives the empirical scaled TTT plot, which can be used to detect the type of hazard rate that the data might have [13]. For example, if the TTT curve is concave (or convex), then the increasing hazard rate (or decreasing hazard rate) class is appropriate. Additionally, if the TTT curve is first concave (or convex) and then convex (or concave), a bathtub (or inverse bathtub) hazard rate should be used. Of course, if the TTT curve is a straight line, the exponential

Table 2
KS and AD p-values and ML estimation of parameters.

Embryo	KS p-value	AD p-value	δ	λ	ξ	γ
ab2	0.895	0.710	0.712 (0.055)	25.575 (10.103)	0.431 (0.477)	0.255 (0.325)
BECab7	0.251	0.311	0.263 (0.027)	1.464 (0.481)	−0.016 (0.011)	−0.235 (0.157)
BECab11	0.984	0.965	1.205 (0.154)	44.222 (41.813)	2.691 (3.115)	0.561 (1.119)
BECac30	0.550	0.874	1.621 (0.322)	58.527 (82.877)	−5.703 (8.945)	0.495 (2.106)
ab18	0.764	0.438	0.910 (0.059)	32.562 (12.193)	2.602 (0.764)	0.279 (0.360)
ac22	0.388	0.320	0.873 (0.058)	28.413 (10.225)	4.100 (0.735)	0.123 (0.330)
ad14	0.244	0.133	0.941 (0.055)	47.262 (16.867)	5.122 (1.005)	0.389 (0.353)
ad22	0.589	0.599	0.940 (0.056)	42.732 (15.851)	1.709 (0.718)	0.709 (0.367)
ad23	0.488	0.349	1.093 (0.106)	26.541 (12.281)	1.950 (1.458)	−0.217 (0.478)
BECab14	0.720	0.546	0.905 (0.093)	26.585 (12.400)	10.931 (1.305)	−0.198 (0.411)
BECab17	0.997	0.999	1.025 (0.129)	13.556 (6.889)	4.527 (0.987)	−0.482 (0.471)
BECab19	0.974	0.992	1.232 (0.157)	27.984 (17.411)	9.896 (2.266)	−0.184 (0.701)
BECad4	0.840	0.626	1.171 (0.324)	19.985 (17.661)	16.361 (4.301)	−1.099 (0.783)
cb16	0.202	0.114	0.802 (0.047)	31.240 (10.268)	4.031 (0.591)	0.300 (0.286)
ab17	0.266	0.076	0.755 (0.031)	33.368 (7.188)	8.322 (0.347)	0.267 (0.185)
ad4	0.490	0.290	0.839 (0.041)	28.524 (6.985)	3.936 (0.541)	−0.009 (0.216)
ad6	0.084	0.040	0.739 (0.038)	22.204 (4.805)	4.190 (0.406)	−0.338 (0.171)
ad16	0.075	0.027	0.798 (0.034)	39.912 (9.347)	5.988 (0.427)	0.448 (0.207)
ad27	0.356	0.186	0.874 (0.052)	22.190 (5.925)	7.786 (0.578)	−0.242 (0.235)
be4	0.023	0.019	0.784 (0.042)	66.974 (16.374)	0.314 (0.368)	0.999 (0.210)
be7	0.074	0.016	0.781 (0.030)	31.599 (6.288)	2.925 (0.337)	0.203 (0.174)
BECab10	0.364	0.342	1.200 (0.107)	133.295 (66.361)	7.231 (1.790)	1.790 (0.571)
BECac12	0.628	0.383	1.073 (0.116)	144.019 (73.295)	2.963 (1.423)	1.964 (0.512)
BECac36	0.419	0.358	1.110 (0.090)	28.292 (11.697)	0.037 (1.302)	−0.101 (0.437)

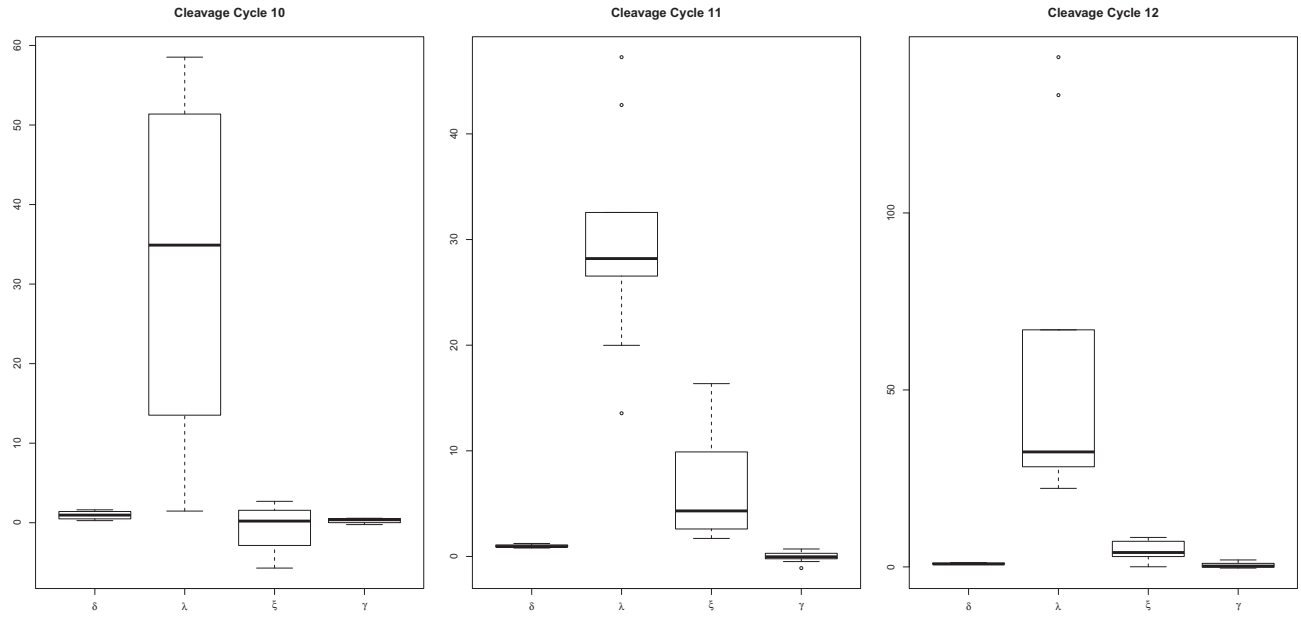

Fig. 3. Box plots for MLE of parameters.

distribution should be employed [13]. More information about TTT function can be found in [19].

3. Empirical results

The quantitative *bcd* gene expression data in wild-type *Drosophila melanogaster* embryos was achieved using FlyEx database [20]. The expression profiles were extracted from the nuclear intensities of %10 longitudinal and are unprocessed for any noise reduction methods. Similar to [21–23], we set to work with A-P data.

Table 2 reports the p-values of KS and AD tests together with ML estimates of parameters achieved in fitting FBS distribution to the actual data for a number of embryos. Overall, the result of the application to real data appears to be consistent with the simulation findings.

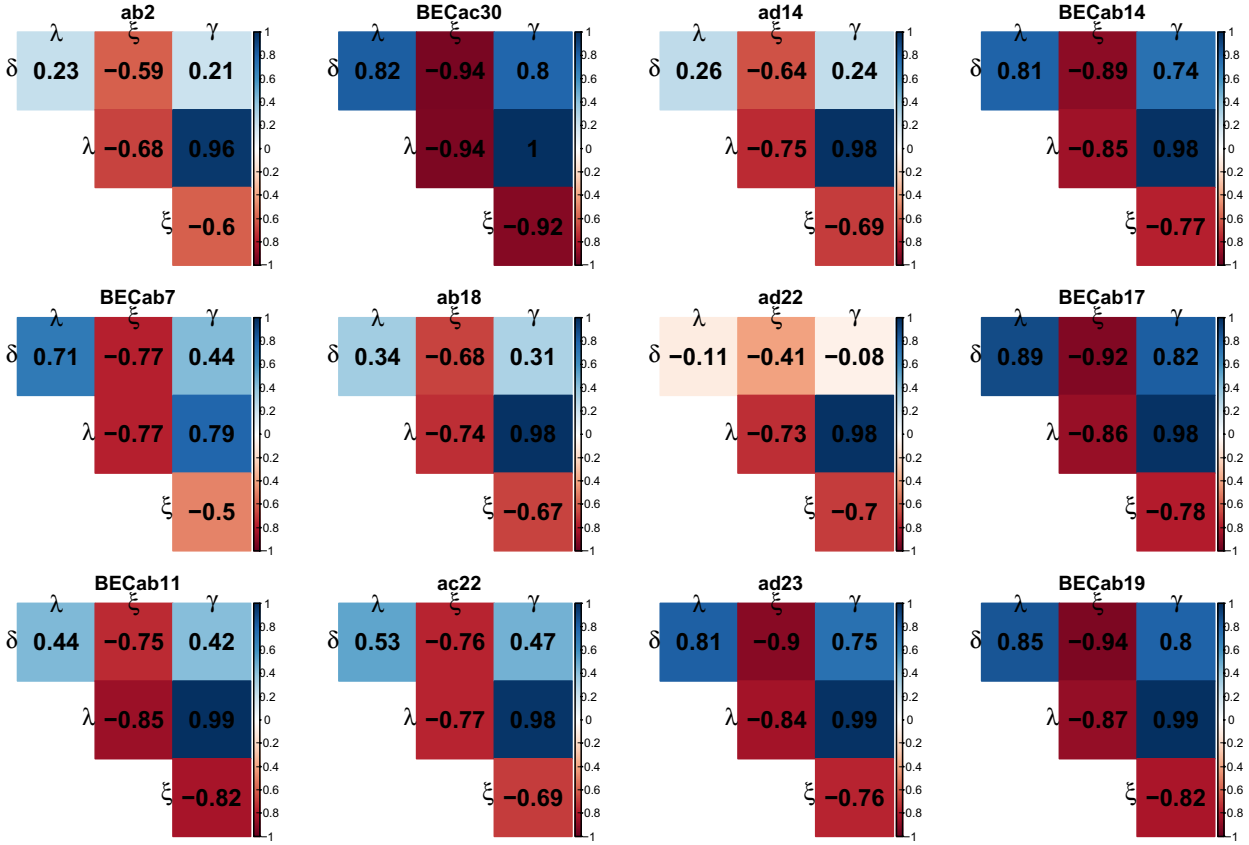

Fig. 4. Correlation for MLE of parameters.

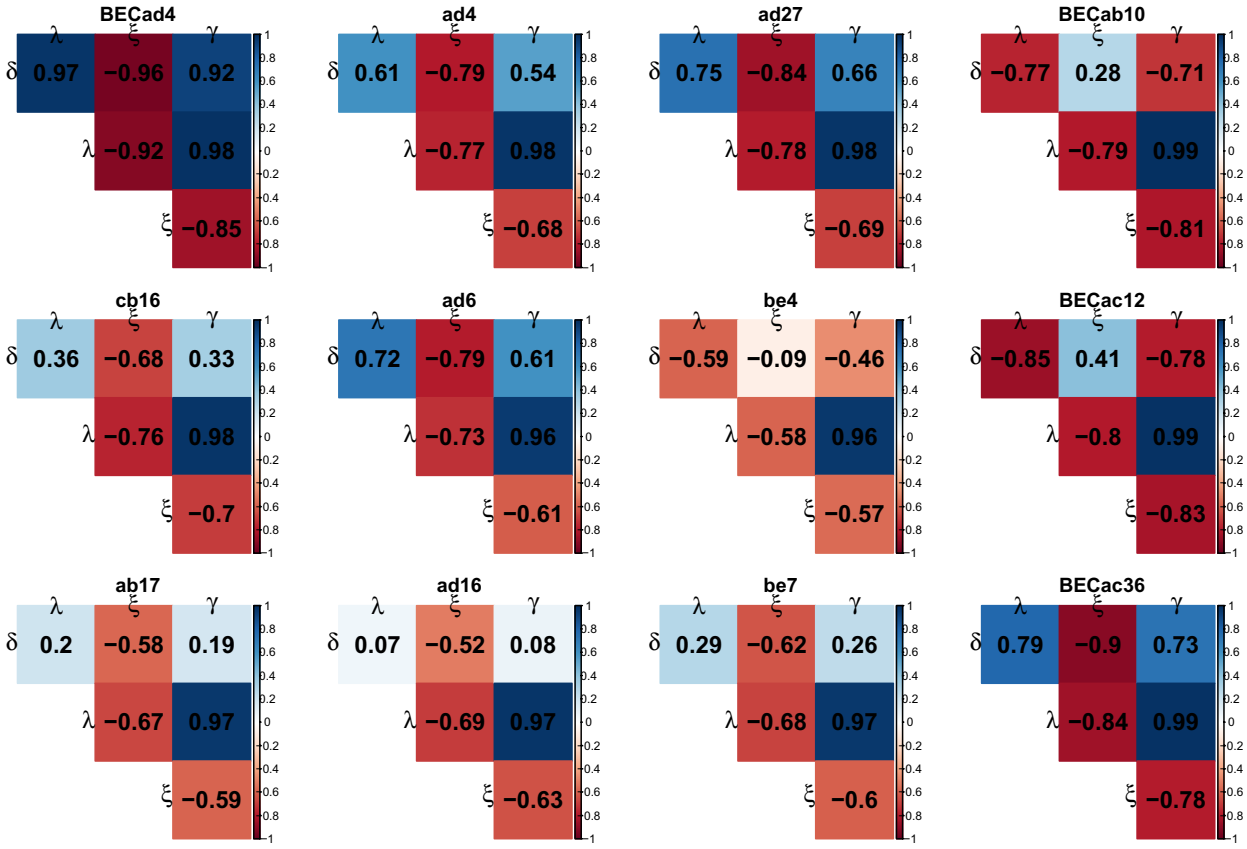

Fig. 5. Correlation for MLE of parameters.

Considering the achieved p-values, it can also be concluded that FBS distribution fits all real data sets at %1 significance level. The standard error of estimation has been reported in parenthesis. As can be seen, in all cases, the largest and smallest standard errors are achieved for the scale (λ) and shape parameter (δ) respectively. Moreover, in most cases, the standard error of location parameter (ξ) is greater than non-centrality parameter (γ).

Fig. 3 depicts the box plot of estimated parameters at three cleavage cycles of 10, 11 and 12. A detailed description of different cleavage cycles is made available in [7]. It is important to highlight that molecules encoded by *bicoid* begin to appear in the embryo at cleavage cycle 10 making the lengths of the *bicoid* profiles of cycles 10 and 11 notably

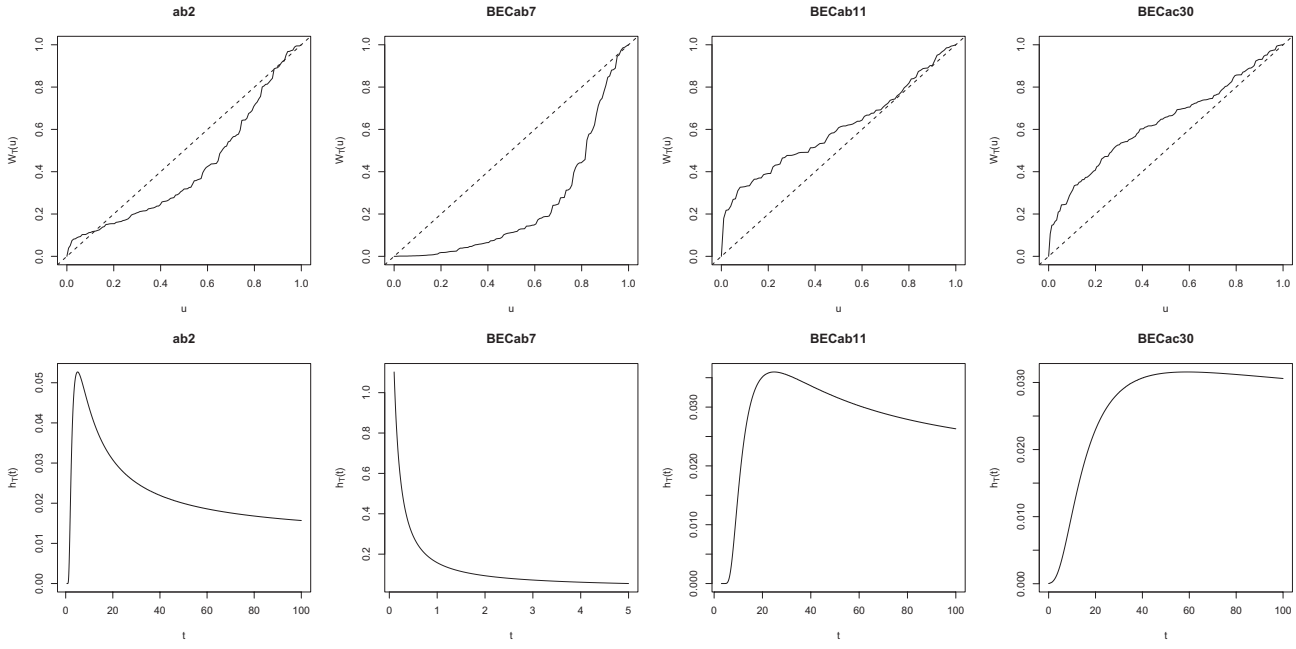

Fig. 6. Empirical scaled TTT plots of embryos in cleavage cycle 10 and corresponding hazard rates.

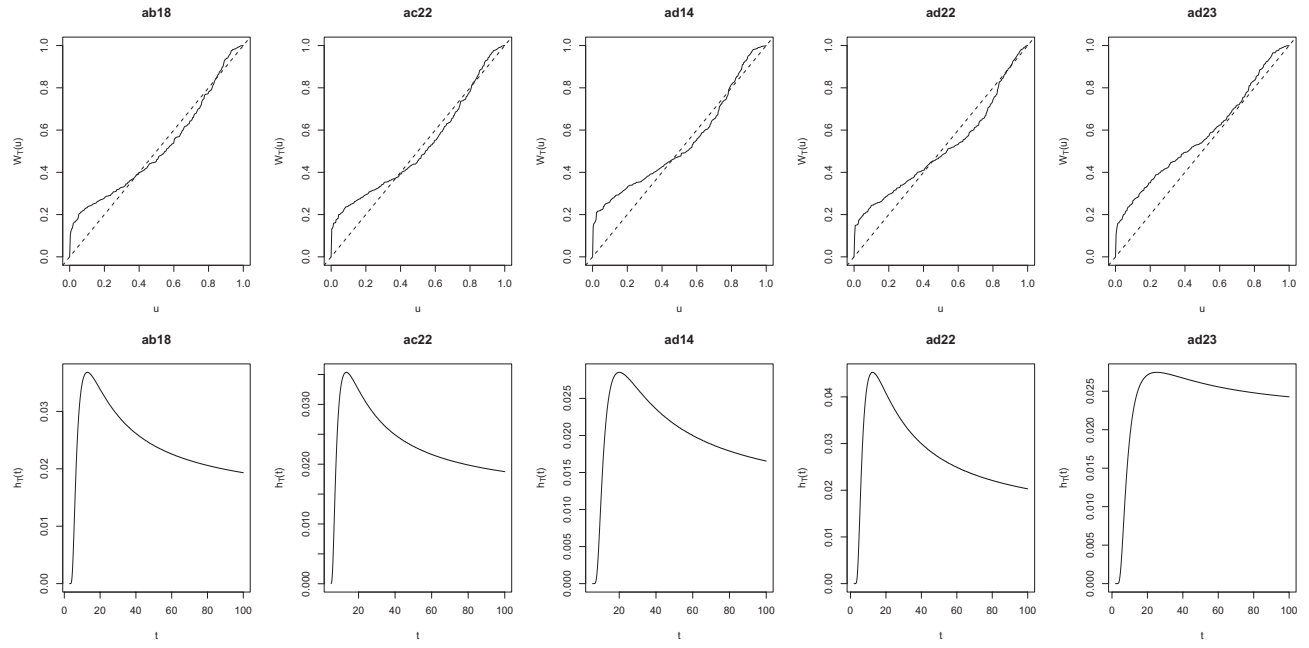

Fig. 7. Empirical scaled TTT plots of embryos in cleavage cycle 11 and corresponding hazard rates (a).

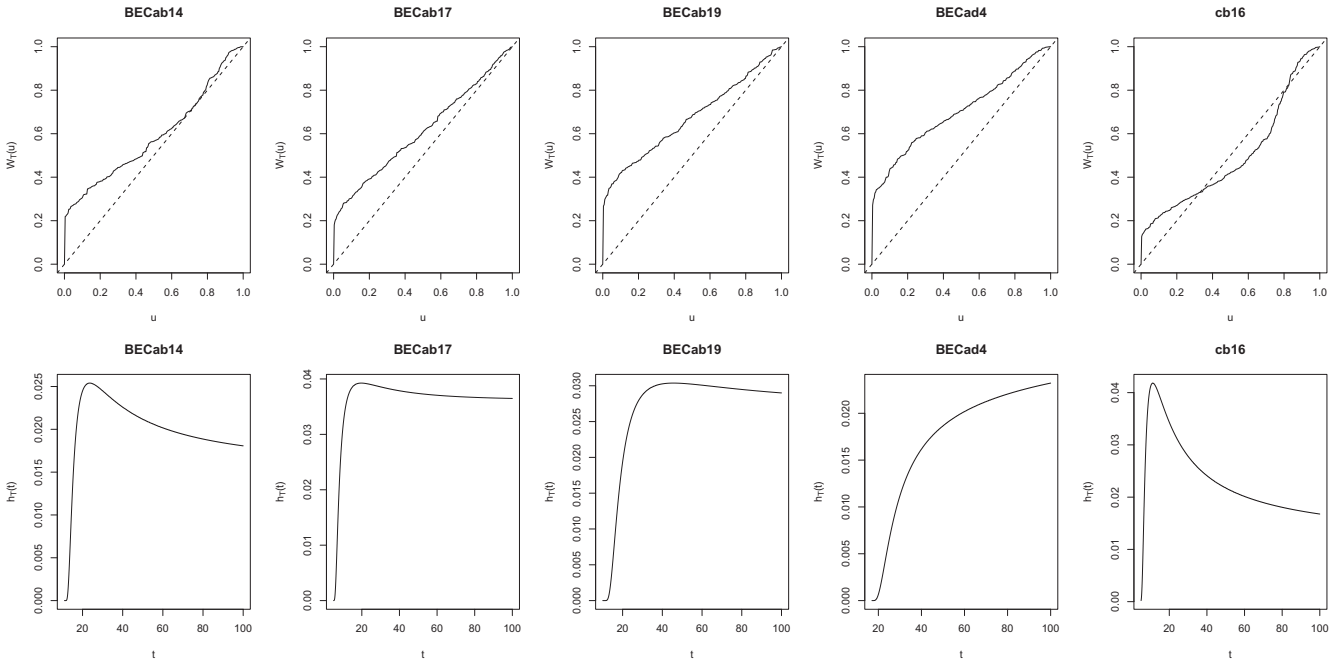

Fig. 8. Empirical scaled TTT plots of embryos in cleavage cycle 11 and corresponding hazard rates (b).

lower than the consequent cycles. Hence, as can be seen, the accuracy of parameter estimation in particular for the scale parameter (λ) is inversely related to the length of available profiles.

Figs. 4 and 5 show the correlation plots for MLE of parameters computed numerically using Hessian matrix at three cleavage cycles of 10, 11 and 12. As can be seen in these figures, there is evidence of a high positive correlation between MLE of $\lambda$and γ in all emberyos. Moreover, the parameter ξ has negative correlation with other parameters in most of cases.

In Figs. 6–10, the empirical scaled TTT plots of all embryos along with hazard rates of corresponding FBS distribution based on ML estimates of parameters δ, λ, ξ and γ (reported in Table 2) are depicted. As can be seen in these figures, the empirical scaled TTT plots have been able to detect the shape of hazard rates well. In cleavage cycle 10, the hazard rate of embryo *BECab7* is decreasing. However, the shape of almost all hazard rates in cleavage cycles 11 and 12 are upside-down bathtub.

4. Conclusion

BS is a right-skewed distribution which has considerable application in modelling a failure over time. Therefore, proposing a more advanced version of this distribution to model the *bicoid* profile correctly matches the nature and the practice of this distribution [24]. Hence, in this paper, BS distribution with four parameters has been put forward to model the *bicoid* gene expression profile.

To obtain the ML estimates of parameters, log-likelihood equations have been proposed, and since there are no explicit solutions to these

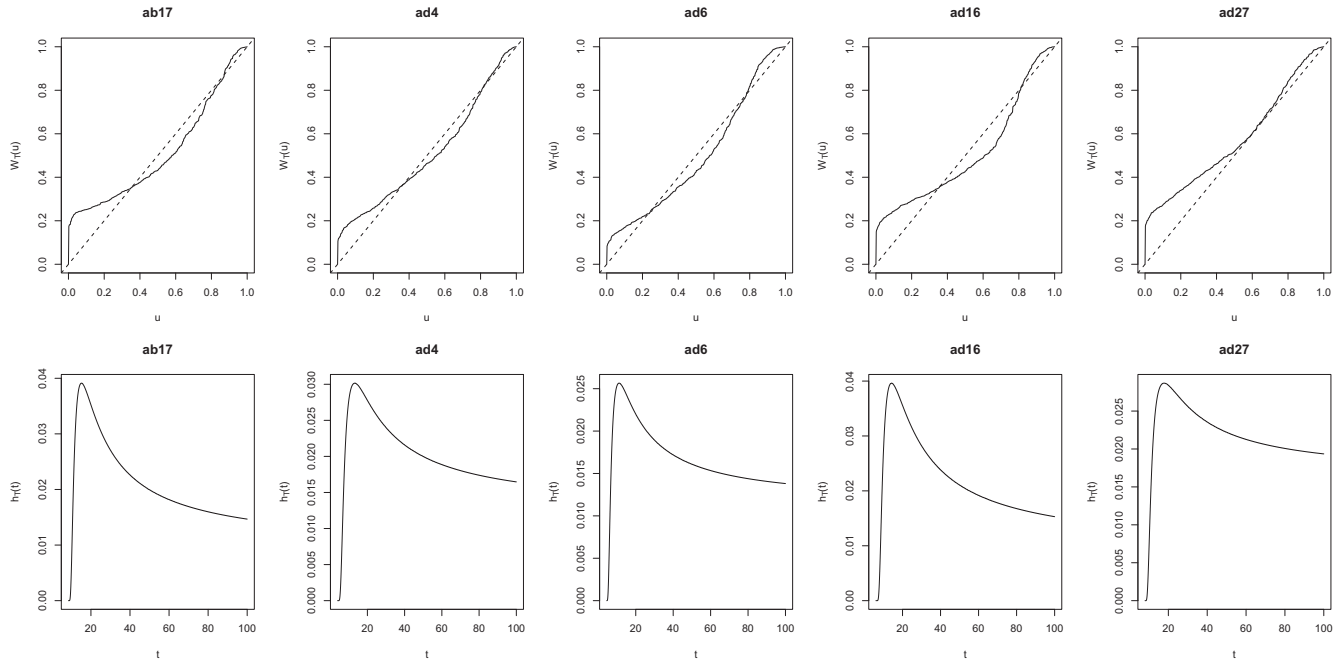

Fig. 9. Empirical scaled TTT plots of embryos in cleavage cycle 12 and corresponding hazard rates (a).

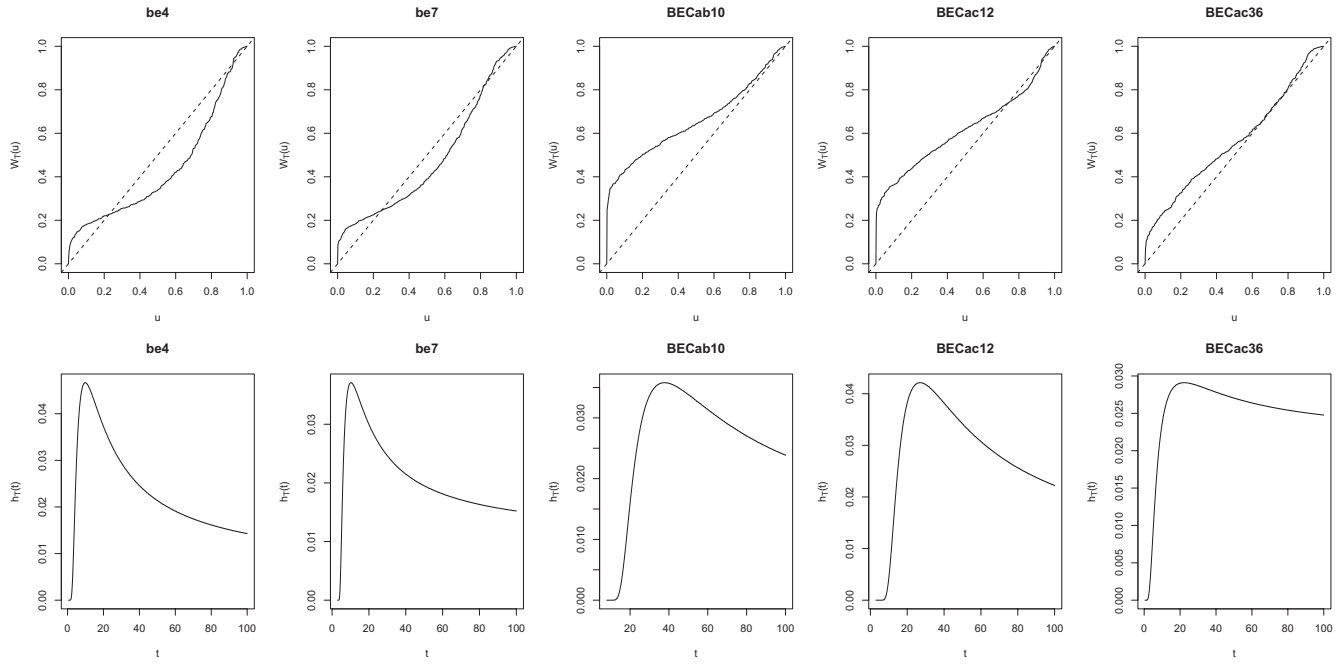

Fig. 10. Empirical scaled TTT plots of embryos in cleavage cycle 12 and corresponding hazard rates (b).

equations due to their non-linearity and complicated form, the ML estimates of four parameters have been achieved numerically.

To assess the newly proposed distribution a simulation step has been performed by simulating the exponential curve drawn from the SDD model as the benchmark. According to the simulation results, the FBS distribution fits the simulated profiles reliably. Also, the results of fitting FBS distribution to real Bcd expression profiles indicate that this distribution performs well on the real data as well.

The comprehensive comparison study performed in [7] and the reliability of the estimated parameters in the current research expect to open up the possibility of using statistical distributions to represent the characteristics of gene expression profiles and unveil the interaction networks in a dynamic multivariate system.

Conflict of interest

None.

Appendix A. Supplementary data

Supplementary data associated with this article can be found, in the online version, athttps://doi.org/10.1016/j.mehy.2018.10.023.

References

[1] Birnbaum ZW, Saunders SC. A new family of life distributions. J Appl Probab 1969;6:319–27.

[2] Leiva V, Barros M, Paula GA, Galea M. Influence diagnostics in log-Birnbaum-Saunders regression models with censored data. Comput Statist Data Anal 2007;51:5694–707.
[3] Barros M, Paula GA, Leiva V. A new class of survival regression models with heavy-tailed errors: robustness and diagnostics. Lifetime Data Anal 2008;14:316–32.
[4] Kundu D, Kannan N, Balakrishnan N. On the hazard function of Birnbaum-Saunders distribution and associated inference. Comput Statist Data Anal 2008;52:2692–702.
[5] Podlaski R. Characterization of diameter distribution data in near-natural forests using the Birnbaum-Saunders distribution. Can J Forest Res 2008;18:518–26.
[6] Lio YL, Park C. A bootstrap control chart for Birnbaum-Saunders percentiles. Qual Reliability Eng Int 2008;24:585–600.
[7] Hassani H, Ghodsi Z. Evaluating the analytical distribution of bicoid gene expression profile. Meta Gene 2017;14:91–9.
[8] Held Jr LI. Deep Homology?: uncanny similarities of humans and flies uncovered by Evo-devo. Cambridge University Press; 2017.
[9] Porcher A, Dostatni N. The bicoid morphogen system. Current Biol 2010;20(5):R249–54.
[10] Pandey UB, Nichols CD. Human disease models in Drosophila melanogaster and the role of the fly in therapeutic drug discovery. Pharmacolog Rev 2011;63(2):411–36.
[11] Muller GB, Wagner GP. Homology, Hox genes, and developmental integration. Am Zool 1996;36(1):4–13.
[12] Akam M. Hox and HOM: homologous gene clusters in insects and vertebrates. Cell 1989;57(3):347–9.
[13] Athayde E, Azevedo C, Leiva V, Sanhueza A. About Birnbaum-Saunders distributions based on the Johnson system. Commun Stat Theor Methods 2012;41:2061–79.
[14] Driever W, Nüsslein-Volhard C. The bicoid protein determines position in the Drosophila embryo in a concentration-dependent manner. Cell 1988;54(1):95–104.
[15] Bergmann S, Sandler O, Sberro H, Shnider S, Schejter E, Shilo BZ, Barkai N. Pre-steady-state decoding of the Bicoid morphogen gradient. PLoS Biol 2007;5(2). [e46].
[16] Houchmandzadeh B, Wieschaus E, Leibler S. Establishment of developmental precision and proportions in the early Drosophila embryo. Nature 2002;415(6873):798–802.
[17] Gregor T, Bialek W, van Steveninck RRDR, Tank DW, Wieschaus EF. Diffusion and scaling during early embryonic pattern formation. Proc Nat Acad Sci USA 2005;102(51):18403–7.
[18] Leiva V. The Birnbaum-Saunders distribution. Elsevier: Academic Press; 2016.
[19] Aarset MV. How to identify a bathtub hazard rate. IEEE Trans Reliab 1987;36:106–8.
[20] Pisarev A, Poustelnikova E, Samsonova M, Reinitz J. FlyEx, the quantitative atlas on segmentation gene expression at cellular resolution. Nucl Acids Res 2009;37(suppl 1):D560–6.
[21] Hassani H, Ghodsi Z. Pattern recognition of gene expression with singular spectrum analysis. Med Sci 2014;2(3):127–39.
[22] Ghodsi Z, Silva ES, Hassani H. Bicoid signal extraction with a selection of parametric and nonparametric signal processing techniques. Genomics Proteomics Bioinf 2015;13(3):183–91.
[23] Ghodsi Z, Hassani H, McGhee K. Mathematical approaches in studying bicoid gene. Quantitative Biol 2015;3(4):182–92.
[24] Fuqiang W, Weixing Y. A model of the fatigue life distribution of composite laminates based on their static strength distribution. Chinese J Aeronaut 2008;21(3):241–6.